Earthquake Engineering, Tenth World Conference © 1992 Balkema, Rotterdam. ISBN 90 5410 060 5

Monotonic axial compression test on ultra-high-strength concrete tied columns

T. Nagashima, S. Sugano, H. Kimura & A. Ichikawa
Takenaka Corporation, Japan

ABSTRACT: To assess the behavior of columns of high strength concrete (HSC) and ultra-high strength concrete (UHSC), twenty-six specimens laterally reinforced with high or ultra-high strength steel bars were tested under monotonic axial loading. Complex tie configurations were used. High strength longitudinal reinforcing bars were also provided. Based on the test results, an analytical model of a stress-strain curve for confined concrete was developed. The proposed model satisfactorily predicted the experimental stress-strain curves for concrete strength up to 1200kg/cm² (118 MPa).

1 INTRODUCTION

The use of high strength concrete which permits smaller cross sections, reduced dead loads, and longer spans has been getting more popular in tall buildings. However, there has been little research on the behavior of high strength concrete columns laterally reinforced with complex square ties and subjected to compressive loading. Twenty six specimens having concrete strength up to 1200 kg/cm² (118 MPa) were tested under monotonic axial loading. While definitions vary, high strength concrete(HSC) may be defined as that having compressive strength in the range from 500 to 1000 kg/cm² (49 to 98 MPa) and ultra-high strength concrete (UHSC)higher than 1000 kg/cm² (98 MPa).

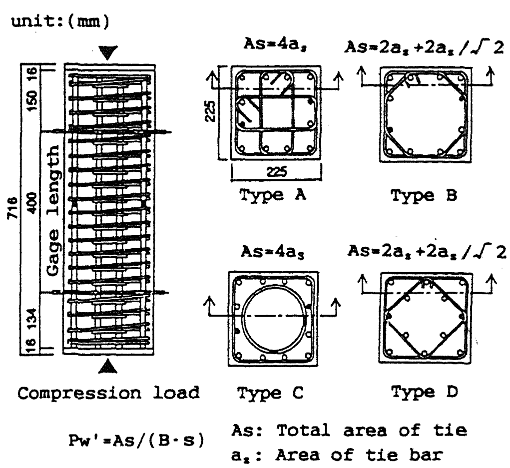

Fig.1 Details of specimen

2 TEST PROGRAM AND SPECIMENS

Specimens, 716 mm long prisms with a 225 mm square cross section as shown in Figure 1, were cast vertically. Normal weight high strength concrete (HSC) and ultra-high strength concrete (UHSC) with specified compressive strength of 600 kg/cm² (59MPa) and 1200 kg/cm² (118MPa), respectively, were used. The maximum size of the coarse aggregate was 10 mm. The thickness of the cover measured from outside of the perimeter tie was kept constant at 10 mm for all specimens. Four different configurations were used for the lateral reinforcement, as shown in Figure 1. High or ultra-high strength steel bars with yield strengths of 8000 and 14000 kg/cm² (784 and 1372 MPa) were used for the ties. It should be noted that high strength bars were closed using a butt weld. For ultra-high strength *bars, outer (perimeter) square spiral* ties and sub-ties with 135° bends extending for 8 bar diameters were provided. Twelve deformed bars with nominal diameter of 10 mm (12-D10) were primarily used for the longitudinal reinforcement. For some specimens with high strength longitudinal bars, the number of the bars was reduced to eight and six. Table 1 gives the properties of

Table 1 Details of test specimens

Specimen	Longitudinal Bars: Number & Size	Longitudinal Bars: Yield Strength fy (kg/cm2)	Lateral Reinforcement: Area Ratio Pw'	Lateral Reinforcement: Volume. Ratio Ps	Lateral Reinforcement: Yield Strength fyh (kg/cm2)	Lateral Reinforcement: Pw'fyh (kg/cm2)	Lateral Reinforcement: Number & Size	Lateral Reinforcement: Spacing s (mm)	Lateral Reinforcement: Config. Type	Concrete(10φ*20mm cylinder): Strength fc' (kg/cm2)	Concrete(10φ*20mm cylinder): Modulus of elast. Ec (kg/cm2)	Concrete(10φ*20mm cylinder): Strain at fc' εo
HH08LA	12-D10	3860	.0071	.0162	14142	100.87	4-U5.1	55	A	1185	377000	.00349
HH10LA	12-D10	3860	.0087	.0198	14142	123.14	4-U5.1	45	A	1185	377000	.00349
HH13LA	12-D10	3860	.0112	.0255	14142	158.46	4-U5.1	35	A	1185	377000	.00349
HH15LA	12-D10	3860	.0133	.0305	13940	185.84	4-U6.4	45	A	1185	377000	.00349
HH20LA	12-D10	3860	.0171	.0392	13940	239.00	4-U6.4	35	A	1204	376000	.00347
HL06LA	12-D10	3860	.0087	.0198	8225	71.62	4-5φ	45	A	1204	376000	.00347
HL08LA	12-D10	3860	.0112	.0255	8225	92.16	4-5φ	35	A	1204	376000	.00347
LL05LA	12-D10	3860	.0069	.0162	8225	56.91	4-5φ	55	A	615	326000	.00293
LL08LA	12-D10	3860	.0112	.0255	8225	92.16	4-5φ	35	A	615	326000	.00293
LH08LA	12-D10	3860	.0069	.0162	14142	97.84	4-U5.1	55	A	615	326000	.00293
LH13LA	12-D10	3860	.0112	.0255	14142	158.46	4-U5.1	35	A	615	326000	.00293
HH13MA	12-D10	6084	.0112	.0255	14142	158.46	4-U5.1	35	A	1204	376000	.00347
HH13HA	12-D10	8197	.0112	.0255	14142	158.46	4-U5.1	35	A	1204	376000	.00347
LL08MA	12-D10	6084	.0112	.0255	8225	92.16	4-5φ	35	A	615	326000	.00293
LL08HA	12-D10	8197	.0112	.0255	8225	92.16	4-5φ	35	A	615	326000	.00293
LH15LA	12-D10	3860	.0133	.0305	13940	185.84	4-U6.4	45	A	628	333000	.00293
HH13LB	12-D10	3860	.0124	.0255	14142	175.17	U5.1	27	B	1204	376000	.00347
HH13LC	12-D10	3860	.0185	.0255	14142	261.40	U5.1&6.4	28	C	1204	376000	.00347
HH13LD	12-D10	3860	.0134	.0255	14142	189.17	U5.1	25	D	1204	376000	.00347
LL08LB	12-D10	3860	.0124	.0255	8225	101.88	5φ	27	B	628	333000	.00293
LL08LC	12-D10	3860	.0169	.0255	8225	138.80	5φ	23	C	628	333000	.00293
LL08LD	12-D10	3860	.0134	.0255	8225	110.02	5φ	25	D	628	333000	.00293
HH13MSA	8-D10	6084	.0112	.0255	14142	158.46	4-U5.1	35	A	1204	376000	.00347
HH13HSA	6-D10	8197	.0112	.0255	14142	158.46	4-U5.1	35	A	1204	376000	.00347
LL08MSA	8-D10	6084	.0112	.0255	8225	92.16	4-5φ	35	A	628	333000	.00293
LL08HSA	6-D10	8197	.0112	.0255	8225	92.16	4-5φ	35	A	628	333000	.00293

the specimens. Primary variables were

1) compressive strength of concrete,

2) capacity of lateral reinforcement ($P_w' \cdot f_{yh}$) in which P_w'= area ratio of lateral reinforcement ; and f_{yh}= yield strength of lateral reinforcement. Pw' is defined as As/(B·s) in which As= total area of lateral reinforcement (see figure 1); B= the center to center distance of a perimeter tie around the square core; and s= the center to center spacing of tie.

3) yield strength of longitudinal reinforcement; 4000, 6000 and 8000 kg/cm² (392, 588 and 784 MPa) and

4) hoop tie configuration ; , , and (Type A, B, C and D).

Except for , all the specimens had the same volumetric ratio of lateral reinforcement.

Monotonic axial compression was applied up to failure by a universal test machine with 1000 t capacity. In all of the specimens, longitudinal strains were measured using displacement transducers over the central 400 mm gage length on two vertical faces of the specimens.

3 BEHAVIOR OF SPECIMENS

Table 2 gives relevant test results and Figure 2 shows an example of final appearance of a specimen. For most specimens, the following events were observed in order during the test : ① yielding of longitudinal reinforcement,

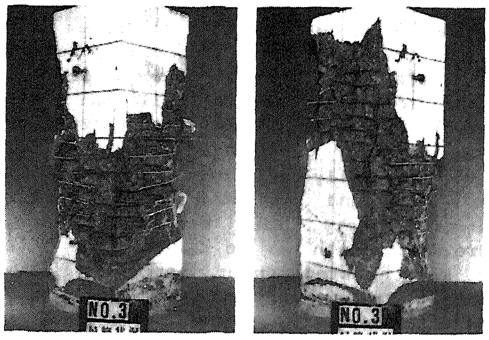

Fig.2 Final appearance of specimen(HH13LA)

② crushing of cover concrete,③ maximum strength of the specimen, and ④ yielding of lateral reinforcement. However, for HSC and UHSC specimens with the largest amount of lateral reinforcement ; LH15LA and HH20LA, the lateral reinforcement yielded ④ before the strength was reached ③. For specimens with high strength longitudinal reinforcement (yield strength of 8000kg/cm² ; 784 MPa), crushing ② occurred before the longitudinal steel yielded ①. All the UHSC specimens failed by slipping of concrete along a diagonal through the column. Buckling of longitudinal reinforcement and fracture of lateral reinforcement were observed along the failure zone.

Table 2 Test results

Specimen	Maximum Stress in Core fcc (kg/cm2)	Strain at fcc εcm	Strain at 85% of fcc ε85	Strain at 50% of fcc ε50	Stress Gain of Core fcc-fc'' (kg/cm2)	Strength of Plain Concrete (=0.85fc') fc'' (kg/cm2)	Effective Capacity of Tie χ·Pw'fyh (kg/cm2)	Ratio of maximumum strength of core to maximum strength of plain concrete Ks (fcc / fc") measured	proposed model	Sheikh et al.	Mander et al.
HH08LA	1251.8	.0044	.0074	.0135	244.6	1007.3	62.5	1.243	1.246	1.213	1.393
HH10LA	1248.7	.0037	.0088	.0146	241.4	1007.3	80.8	1.240	1.280	1.249	1.490
HH13LA	1341.0	.0055	.0119	.0209	333.7	1007.3	109.9	1.331	1.327	1.299	1.632
HH15LA	1294.8	.0089	.0183	.0349	287.6	1007.3	122.0	1.285	1.344	1.307	1.692
HH20LA	1511.0	.0171	.0233	.0335	487.6	1023.4	165.8	1.476	1.395	1.363	1.867
HL06LA	1204.9	.0043	.0083	.0167	181.5	1023.4	46.1	1.177	1.208	1.183	1.295
HL08LA	1358.0	.0038	.0067	.0132	334.6	1023.4	62.8	1.327	1.243	1.220	1.388
LL05LA	701.8	.0036	.0088	.023	179.1	522.8	34.6	1.343	1.353	1.307	1.416
LL08LA	808.8	.0076	.0125	.0267	286.1	522.8	62.8	1.547	1.476	1.431	1.682
LH08LA	723.2	.0057	.0167	.0354	200.5	522.8	60.6	1.383	1.468	1.410	1.665
LH13LA	873.0	.0116	.0259	.0358	350.3	522.8	109.9	1.670	1.630	1.577	2.044
HH13MA	1343.5	.0048	.0092	.0159	320.1	1023.4	109.9	1.313	1.322	1.295	1.624
HH13HA	1317.0	.0042	.0118	.0223	293.6	1023.4	109.9	1.287	1.322	1.295	1.624
LL08MA	811.3	.009	.0133	.0229	288.6	522.8	62.8	1.552	1.476	1.431	1.682
LL08HA	794.7	.0099	.015	.0307	271.9	522.8	62.8	1.520	1.476	1.431	1.682
LH15LA	904.0	.0223	.04	.04	370.2	533.8	122.0	1.693	1.650	1.580	2.114
HH13LB	1342.7	.0064	.0096	.0227	319.3	1023.4	125.1	1.312	1.343	1.303	1.692
HH13LC	1302.1	.0036	.0094	.0224	278.7	1023.4	108.0	1.272	1.319	1.160	1.615
HH13LD	1307.0	.0038	.0092	.0239	283.6	1023.4	122.9	1.277	1.340	1.272	1.682
LL08LB	839.7	.007	.0088	.0228	305.9	533.8	72.7	1.573	1.502	1.442	1.754
LL08LC	761.3	.004	.0087	.0279	227.5	533.8	58.9	1.426	1.452	1.240	1.637
LL08LD	787.4	.0041	.0138	.0357	253.6	533.8	71.5	1.475	1.497	1.397	1.743
HH13MSA	1322.3	.0038	.0107	.0169	298.9	1023.4	109.9	1.292	1.322	1.251	1.620
HH13HSA	1374.9	.00438	.0148	.0274	351.5	1023.4	109.9	1.343	1.322	1.162	1.618
LL08MSA	804.9	.0104	.0147	.029	271.1	533.8	62.8	1.508	1.466	1.349	1.667
LL08HSA	820.6	.0091	.0144	.0307	286.8	533.8	62.8	1.537	1.466	1.209	1.665

4 STRESS-STRAIN RELATIONSHIP OF CONFINED CORE CONCRETE

To obtain the relationship between stress and strain in the core concrete, the contributions of longitudinal steel and cover were subtracted from the total applied load. It was assumed that the maximum strength (fc'') and the strain at the maximum stress (ε_m) of the cover and unconfined concrete were equal to 0.85fc' and ε_0, in which fc' and ε_0 were the compressive strength and the strain at maximum stress measured from $100\phi \times 200$ mm cylinder test. After the strength was reached, the stress was assumed to be zero. The ascending part of the stress-strain curve of plain concrete was represented by a parabola for HSC and a straight line for UHSC. Stress-strain curve of the longitudinal steel was assumed to be bilinear.

Figure 3(a) and (b) show stress-strain curves of specimens with different amounts of lateral reinforcement and other parameters constant (concrete strength, tie configuration and strength of longitudinal steel). For the UHSC Specimens with $P_w' \cdot f_{yh} < 186$ kg/cm² (18.2 MPa), the load dropped suddenly at a strain smaller than 1 % . The specimens with $P_w' \cdot f_{yh} \geq 186$ kg/cm² (18.2 MPa) maintained load carrying capacity up to a strain larger than 2 % . The HSC specimens with $P_w' \cdot f_{yh} \geq 92$ kg/cm² (9.0 MPa) exhibited satisfactory behavior. In comparisons between the specimens with the same value of $P_w' \cdot f_{yh}$ but different concrete strengths, the compressive ductilities in the HSC specimens were larger than those in the UHSC specimens.

Close tie spacing resulted in an increase in the strength of core concrete even though the tie configuration and the capacity of lateral reinforcement, Pw'·f_{yh}, were the same. However, compression ductility showed little difference in these specimens.

Comparison of stress-strain curves of core concrete with different tie shape but with equal amounts of longitudinal and lateral steel are shown in figure 3 (c) and (d).

Specimens with configurations and showed slightly larger gain in strength and ductility than that with configurations and for both HSC and UHSC.

High strength longitudinal bars with yield strengths approximately 1.5 and 2.0 times that of normal strength bars, had little effect on strength and ductility of the confined core concrete when the same tie shape and an equal amount of longitudinal steel were used.

There was no major difference in the strength and ductility for both HSC and UHSC specimens with twelve, eight and six longitudinal bars, with the exception of the UHSC specimen with six longitudinal bars which exhibited the largest ductility.

5 ANALYTICAL MODEL FOR CONFINED CONCRETE

Stress-strain curves obtained from the test and analytical models which were proposed by Sheikh & Uzumeri[1982] and Mander [1988] are shown in figure 4.

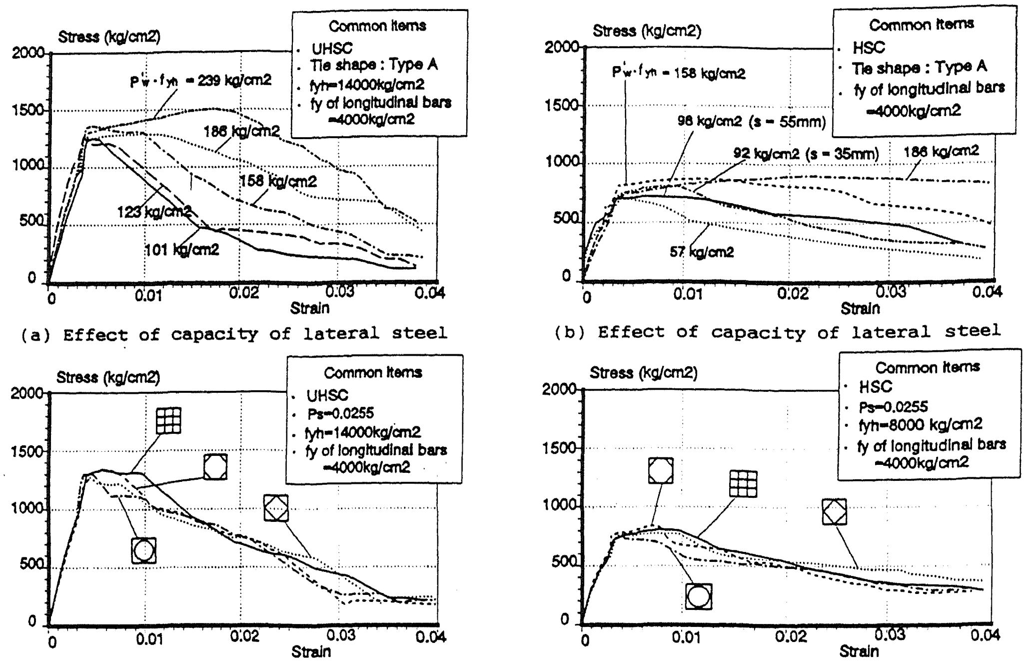

(a) Effect of capacity of lateral steel

(b) Effect of capacity of lateral steel

(c) Effect of tie configuration

(d) Effect of tie configuration

Fig.3 Comparison of stress-strain curves

The ratios of maximum strength of core to maximum strength of plain concrete (Ks) for each model are listed in Table 2. The Sheikh & Uzumeri model shows good agreement with maximum strengths for both UHSC and HSC specimens, however strains at maximum strength and descending parts of the curves are different from measured curves, especially for UHSC specimens. The Mander model overestimates maximum strengths and strains at maximum strength, and differences on the descending part of the curve are significant. Both models do not estimate appropriately the strain at the maximum strength and the ductility for HSC and UHSC. Therefore an analytical model for HSC and UHSC was developed. For the ascending part of the curve, an expression used by Mander was used as follows.

For $0 < \varepsilon_c \leq \varepsilon_{cm}$

$$fc = fcc \cdot x \cdot r/(r-1+x^r) \qquad (1)$$

where $x=\varepsilon_c/\varepsilon_{cm}$; $r= Ec/(Ec - Esec)$ and $Esec = fcc / \varepsilon_{cm}$

For $\varepsilon_{cm} < \varepsilon_c$

$$fc = fcc\left[1 - 0.5\,\frac{\varepsilon_c - \varepsilon_{cm}}{\varepsilon_{50} - \varepsilon_{cm}}\right] \geq 0.3f_{cc} \qquad (2)$$

where fc = longitudinal stress in concrete (kg/cm^2); ε_c = longitudinal strain in concrete; fcc = maximum stress in confined concrete (kg/cm^2), (given in Eq.(4) later); ε_{cm}= strain at maximum stress in confined concrete (given in Eq.(5) later); Ec = tangent modulus of elasticity of plain concrete (kg/cm^2) and ε_{50} = strain at 0.5fcc (given in Eq.(6) later).

5.1 Compressive strength of confined core concrete, fcc

Figure 5(a) shows the increase in compressive strength (fcc-fc'') resulting from confinement as a function of capacity of lateral reinforcement ($Pw' \cdot f_{yh}$). It is likely that the strength gain for a square column with concrete strength up to 1200 kg/cm^2 (118 MPa) increases with $Pw' \cdot f_{yh}$ and does not depend on concrete strength. To take account of tie spacing and tie configuration, effective capacity of lateral reinforcement ($\lambda^* \cdot Pw' \cdot f_{yh}$) was used in which λ^* was a reduction factor proposed by Sheikh & Uzumeri [1982] and was simplified to the following

$$\lambda^* = \left(1 - \frac{\Sigma\ Ci^2}{6B^2}\right)\left(1 - \frac{S}{2B}\right)^2 \qquad (3)$$

where Ci = the center-to-center distance between longitudinal perimeter bars

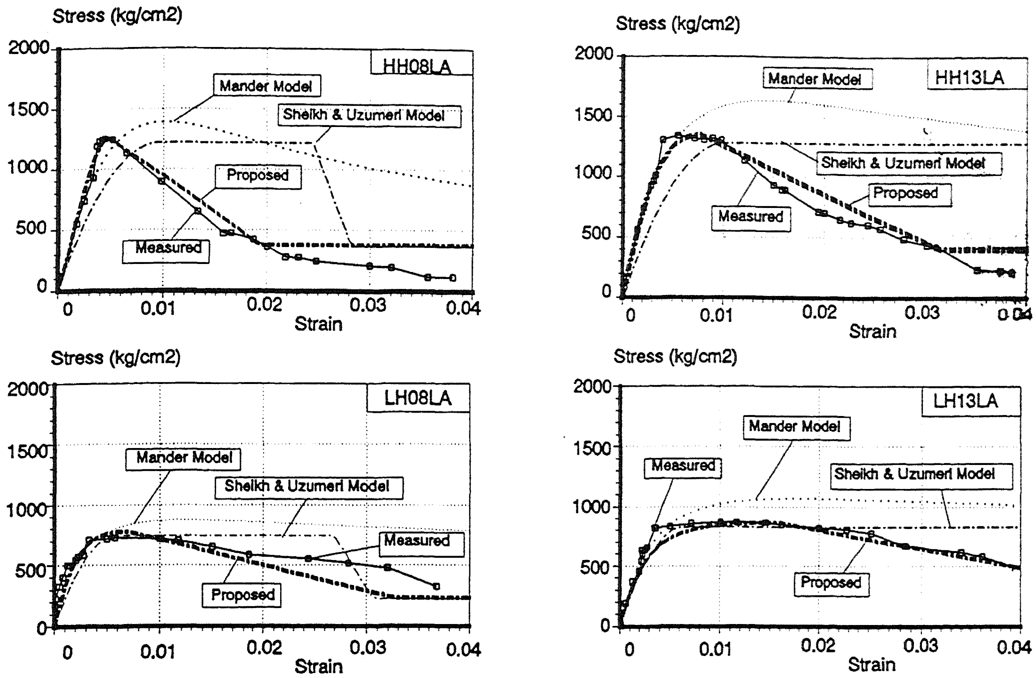

Fig.4 Comparison of measured stress-strain curves and analytical models

B = the center-to-center distance of a perimeter tie around the square core and s = the tie spacing. Figure 5(b) shows the relation between strength gain (fcc-fc'') in confined concrete and effective capacity of lateral reinforcement ($\lambda^{*} \cdot Pw' \cdot f_{yh}$). The best parabolic curve through the data is given by

$$fcc - fc'' = 31.4 \sqrt{\lambda^{*} Pw' \cdot f_{yh}} \qquad (4)$$

where fc''= the strength of unconfined concrete which was assumed to be 0.85fc' in this test. Unit in the equation are (kg/cm^2).

5.2 Strain at maximum stress in confined core concrete, ε_{cm}

The ratio of the strain at maximum strength in confined concrete to that in unconfined concrete ($\varepsilon_{cm} / \varepsilon_{m}$) is plotted as a function of the effective capacity of lateral reinforcement normalized by concrete strength ($\lambda^{*} \cdot Pw' \cdot f_{yh}/fc''$) in Figure 6. The value of $\varepsilon_{cm}/ \varepsilon_{m}$ increases sharply when $\lambda^{*} \cdot Pw' \cdot f_{yh}/fc''$ exceeds 0.1. From regression analysis, the best fit parabola which intercepts the vertical axis at 1.0 was given as follows.

$$\varepsilon_{cm} / \varepsilon_{m} = 138 \, (\lambda^{*} Pw' \cdot f_{yh}/fc'')^2 + 1 \qquad (5)$$

5.3 Ductility in compression

To evaluate the ductility in compression, the strains at 85% and 50% of the maximum strength (ε_{85} and ε_{50}) were selected as listed in Table 2. Both ε_{85} and ε_{50} increased as the effective capacity of lateral reinforcement normalized by concrete strength ($\lambda^{*} \cdot Pw' \cdot f_{yh}/fc''$) was increased. Therefore, specimens with higher strength concrete exhibit lower compression ductility when the capacity of lateral reinforcement is identical. In other words, to get an equal ductility, the specimen with higher strength concrete needs a larger amount of lateral steel.

To determine the descending part of the stress-strain curve, ε_{50} was selected. Because the slope of the descending part is very sensitive for ε_{85}. The following equation for ε_{50} was derived from a regression analysis as shown in Figure 7.

$$\varepsilon_{50} = \varepsilon_{m} + 0.193(\lambda^{*} Pw' \cdot f_{yh}/fc'') \qquad (6)$$

5.4 Comparison of analytical and experimental curves

The proposed model was compared with experimental curves in Figure 4. The agreement observed between the predicted and the experimental behavior of confined concrete is quite good for columns with both HSC and UHSC concrete.

6 CONCLUSION

An experimental program involving HSC and UHSC square columns with complex tie arrangements was conducted. The following conclusions can be drawn from the results of this study;

1) For columns with UHSC of 1200 kg/cm^2 (118 MPa), the capacity of lateral reinforcement normalized by strength of plain concrete ($P_w \cdot f_{yh}/fc''$) higher than 0.18 prevented a sudden failure after the maximum strength was reached and improved compression ductility when the tie configuration was used.

2) Hoop tie configurations and provided slightly larger strength and ductility than and when the same volumetric ratio of lateral reinforcement was used.

3) The strength of longitudinal steel had little effect on the stress-strain relation of the confined concrete.

4) The maximum strength of confined concrete was independent of the number of longitudinal bars when the same tie configuration was used.

5) The maximum stress enhancement of confined concrete from plain concrete was independent of the concrete strength and was proportional to the square root of the effective lateral confinement capacity ($\sqrt{\lambda^* Pw' \cdot f_{yh}}$) .

6) The compression ductility of confined concrete was directly proportional to the capacity of lateral steel and inversely proportional to the concrete strength. Therefore, to provide equal ductility, a column with higher strength concrete needs a larger amount of lateral steel.

7) An analytical model of the stress-strain curve for concrete strength up to 1200 kg/cm^2 (118 MPa) was proposed. The proposed model satisfactorily predicted experimental stress-strain curves.

REFERENCES

Mander, J.B., Priestley, M.J.N. and Park, R. 1988. Theoretical Stress-Strain Model for Confined Concrete. Proceedings, ASCE, Vol.114, No.8, August: 1804-1826.

Sheikh, S.A. and Uzumeri, S.M. 1982. Analytical Model for Concrete Confinement in Tied Columns. Proceedings, ASCE, Vol.108, No. ST12, December: 2703-2722.

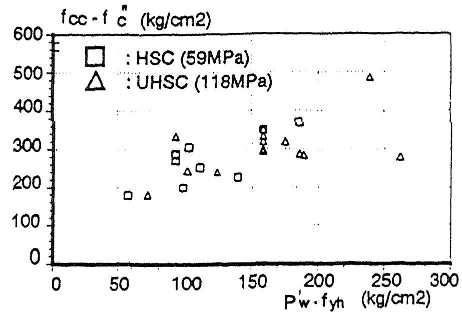

Fig.5(a) Stress gain of confined concrete versus capacity of lateral reinforcement

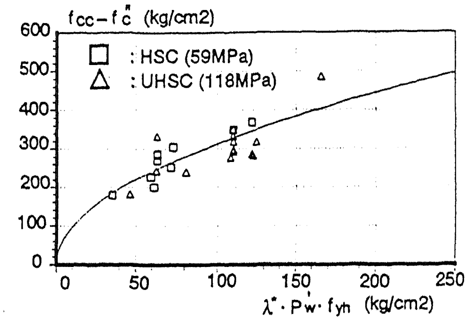

Fig.5(b) Stress gain of confined concrete versus effective capacity of lateral reinforcement

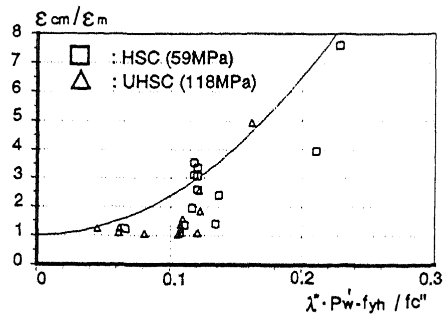

Fig.6 Effect of effective capacity of lateral reinforcement and concrete strength on strain at maximum strength

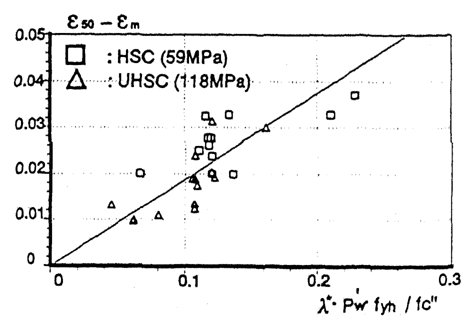

Fig.7 Evaluation of compression ductility